J|A|C|S
ARTICLES
Published on Web 01/13/2006

The A^-F_X to $F_{A/B}$ Step in *Synechocystis* 6803 Photosystem I Is Entropy Driven

Harvey J. M. Hou[†] and David Mauzerall*[,‡]

Contribution from the Department of Chemistry, Gonzaga University, 502 East Boone Avenue, Spokane, Washington 99258, and The Rockefeller University, 1230 York Avenue, New York, New York 10021

Received July 20, 2005; E-mail: mauzera@mail.rockefeller.edu

Abstract: We have previously reported the enthalpy and volume changes of charge separation in photosystem I from *Synechocystis* 6803 using pulsed photoacoustics on the microsecond time scale, assigned to the electron-transfer reaction from excited-state P_{700}* to $F_{A/B}$ iron sulfur clusters. In the present work, we focus on the thermodynamics of two steps in photosystem I: (1) $P_{700}^* \rightarrow A_1^-F_X$ (<10 ns) and (2) $A_1^-F_X \rightarrow F_{A/B}^-$ (20−200 ns). The fit by convolution of photoacoustic waves on the nanosecond and microsecond time scales resolved two kinetic components: (1) a prompt component (<10 ns) with large negative enthalpy (-0.8 ± 0.1 eV) and large volume change (-23 ± 2 A^3), which are assigned to the $P_{700}^* \rightarrow A_1^-F_X$ step, and (2) a component with ~200 ns lifetime, which has a positive enthalpy ($+0.4 \pm 0.2$ eV) and a small volume change (-3 ± 2 A^3) that are attributed to the $A_1^-F_X \rightarrow F_{A/B}^-$ step. For the fast reaction using the redox potentials of A_1F_X (−0.67 V) and P_{700} (+0.45 V) and the energy of P_{700}* (1.77 eV), the free energy change for the $P_{700}^* \rightarrow A_1^-F_X$ step is −0.63 eV, and thus the entropy change ($T\Delta S$, $T = 25$ °C) is -0.2 ± 0.3 eV. For the slow reaction, $A_1^-F_X \rightarrow F_{A/B}^-$, taking the free energy of −0.14 eV [Santabara, S.; Heathcote, P; Evans, C. W. *Biochim. Biophys. Acta* **2005**, *1708*, 283−310], the entropy change ($T\Delta S$) is positive, $+0.54 \pm 0.3$ eV. The positive entropy contribution is larger than the positive enthalpy, which indicates that the A^-F_X to $F_{A/B}^-$ step in photosystem I is entropy driven. Other possible contributions to the measured values are discussed.

Introduction

Photosystem I (PS I) is a pigment−protein complex that consists of at least 11 polypeptides embedded in the photosynthetic membrane. It drives light-induced electron transfer from reduced plastocyanin (or cytochrome c_6) to oxidized ferredoxin (or flavodoxin), generating as its final product NADPH.[1]

The three-dimensional structure of PS I from *Synechococcus elongates* has been provided at 2.5 Å resolution.[2] The precise orientation of pigment and other cofactors and their interaction with protein subunits in PS I are used in structure and function studies. There are two phylloquinone molecules (A_{1A} and A_{1B}) located in the PsaA and PsaB subunits in PS I.[3−5] Based on the structure of PS I, recent kinetic studies with site-directed mutants from *Chlamydomonas* gave evidence for two active electron branches in PS I.[6] However, the contrary view of asymmetric electron transfer in cyanobacteria is still widely supported.[7] Kinetic investigations by means of time-resolved spectroscopic methods have established the main electron-transfer pathway in the PS I reaction center.[8] It is generally believed that (1) upon the absorption of light, the excitation energy is transferred from light-harvesting chlorophylls to the primary donor P_{700} (a pair of chlorophyll *a* molecules) in several hundred femtoseconds; (2) the excited P_{700}* delivers an electron to the primary acceptor A_0 (a chlorophyll *a* monomer) in about 3−14 ps; (3) the reduced A_0^- donates its electron to the secondary acceptor A_1 (a phylloquinone) in approximately 50 ps; (4) A_1^- passes its electron to F_X (an iron sulfur cluster) with two time constants, ~20 and ~200 ns; and (5) finally the reduced F_X^- transfers its electron to F_A and F_B in about 50−200 ns.

A recent review by Santabara, Heathcote, and Evans has summarized the conflicting evidence on this pathway.[9] They conclude that not only must reverse reactions be considered but that the entire sequence is close to isoenergetic, including the A_0 and A_1 along the alternate symmetric pathway. The complex kinetic scheme they propose accounts for the observations, and

[†] Gonzaga University.
[‡] The Rockefeller University.

(1) Chitnis, P. R. *Annu. Rev. Plant Phys. Plant Mol. Biol.* **2001**, *52*, 593−626.
(2) Jordan, P.; Fromme, P.; Witt, H. T.; Klukas, O.; Seanger, W.; Krauss, N. *Nature* **2001**, *411*, 909−917.
(3) Klukas, O.; Schubert, W.-D.; Jordan, P.; Krauss, N.; Fromme, P.; Witt, H. T.; Saenger, W. *J. Biol. Chem.* **1999**, *274*, 7361−7367.
(4) Golbeck, J. H. *Annu. Rev. Biophys. Biomol. Struct.* **2003**, *32*, 237−256.
(5) Bittl, R.; Zech, S. G.; Fromme, P.; Witt, H. T.; Lubitz, W. *Biochemistry* **1997**, *36*, 12001−12004.
(6) (a) Joliot, P.; Joliot, A. *Biochemistry* **1999**, *38*, 11130−11136. (b) Guergova-Kuras, M.; Boudreaux, B.; Joliot, A.; Joliot, P.; Redding, K. *Proc. Natl. Acad. Sci. U.S.A.* **2001**, *98*, 4437−4442.
(7) (a) Ramesh, V. M.; Gibasiewicz, K.; Lin, S.; Bingham, S. E.; Webber, A. N. *Biochemistry* **2004**, *43*, 1369−1375. (b) Cohen, R. O.; Shen, G.; Golbeck, J. H.; Xu, W.; Chitnis, P. R.; Valieva, A. I.; Van der Est, A.; Pushkar, Y.; Stehlik, D. *Biochemistry* **2004**, *43*, 4741−4754. (c) Hastings, G.; Sivakumar, V. *Biochemistry* **2001**, *40*, 3681−3689.
(8) (a) Brettel, K. *Biochim. Biophys. Acta* **1997**, *1318*, 322−373. (b) Brettel, K.; Leibl, W. *Biochim. Biophys. Acta* **2001**, *1507*, 100−14.
(9) Santabara, S.; Heathcote, P.; Evans, C. W. *Biochim. Biophys. Acta* **2005**, *1708*, 283−310.

10.1021/ja054870y CCC: $33.50

the observable time constants are complex functions of those of the individual steps. The average time constant for the $A_1 \leftrightarrow F_X$ to $F_A \leftrightarrow F_B$ partition is close to the step we observe, and we will use their formulation for consistency. We note that none of our conclusions would be altered by the use of the other parameters; only the magnitude of the quoted enthalpies and entropies would be larger.

Thermodynamics of charge-transfer reactions in biological systems are as important as kinetics to fully understand the molecular mechanisms in detail. However, the thermodynamic data are relatively limited. In recent years, the thermodynamic parameters on the microsecond time scale, such as volume changes (ΔV) and enthalpy changes (ΔH) accompanying electron-transfer reactions, have been obtained by means of pulsed time-resolved photoacoustics in chemical solutions and in biological systems,[10−13] especially in photosynthesis.[14−24] Photoacoustic pressure waves at room temperature contain both thermal and intrinsic molecular volume changes produced by thermal expansion and, for example, by charge separation. At ~4 °C in dilute aqueous solution, the thermal signal is null as the thermal expansivity (β) is zero, and thus the intrinsic volume change of reaction can be measured directly. The change of photoacoustic pressure wave signals with temperature can be used to determine the thermal components of the charge-transfer reaction. Assuming the change in Gibbs free energy is given by the difference in redox potentials of the corresponding charge-transfer reactions, the entropy change of the reaction may be calculated using the Gibbs relation. A significant positive entropy change on formation of $P^+Q_A^-$ in the photosynthetic reaction center from *Rb sphaeroides* was found as the change in enthalpy was only about one-half of the change in free energy.[17] Further photoacoustic measurements revealed that the entropy change of electron transfer in PS I trimer from *Synechocystis* sp. PCC 6803 on the microsecond time scale is the same as that in bacterial centers.[18] In contrast, electron transfer in PS II core complexes from *Synechocystis* sp. PCC 6803 is accompanied by a small negative entropy change.[19] These observations were confirmed using intact living cells of the same organism.[20]

The observed thermodynamic parameters in PS I on the 1-μs time scale were assigned to the formation of charge-separated species $P_{700}{}^+F_{A/B}{}^-$ from excited P_{700}*.[18] The time constant of charge transfer from $A_1{}^-$ to $F_{A/B}$ is reported to be 20−200 ns.[25−29] However, the analysis of Santabara et al. indicates complex equilibria between the various species.[9] The enthalpy and volume changes associated with this reaction and with the charge separation of the $P_{700}* \rightarrow A_1$ reaction seem unknown, so we investigated these reactions by fast pulsed photoacoustics on the nanosecond time scale. Unexpectedly and strikingly, a larger enthalpy change was observed by the peak-to-peak PA (photoacoustic(s)) analysis on this time scale than that observed on the microsecond time scale. Convolution of photoacoustic signals on nanosecond and microsecond time scales resolved enthalpy and volume changes of two steps and produced a positive enthalpy for the second step. The results indicate that the entropy is the driving force in the charge-transfer step forming $P_{700}{}^+F_{A/B}{}^-$ from $P_{700}{}^+A_1{}^-F_X$. Such reactions are of interest because, unlike most chemical reactions, which are driven by changes in bond energy or similar energetic processes, these are driven by the increased probability of the reaction. Systems that allow large changes in degrees of freedom, such as proteins, are the most likely to show this property.

Experimental Procedures

Preparation of Purified PS I Trimers. PS I trimers were isolated from *Synechocystis* sp. PCC 6803 and purified according to published methods.[30−31] For PA measurements, the sample buffer was replaced by ultrafiltration over a Centriprep YM-50 membrane with pH 8.0, 10 mM *N*-[2-hydroxyethyl]piperazine-*N*′-2-ethanesulfonic acid (HEPES), and 0.03% dodecyl-α-D-maltoside (DM) without sucrose or glycerol.

Fast Photoacoustic Measurements. The fast pulsed time-resolved photoacoustic setup on the nanosecond time scale is similar to that on the microsecond time scale,[17−19] except the photoacoustic cell path is 0.10 mm instead of 1.0 mm. In brief, the light beam was produced by a Nd:YAG laser (Surelite) and an optical parametric oscillator (OPO, Surelite). An excitation wavelength of 680 nm was selected to excite the PS I centers. The PA cell consisted of a 5 mm methacrylate window, a 0.10 mm spacer, a dielectric mirror (99% reflection, Newport), and a piezo-film (28 μ). The mirror (5 mm thickness) delays the measured photoacoustic signal (~1 μs) and eliminates possible electric or light artifacts produced by laser pulses. The voltage produced by the piezo-film was amplified and filtered (Ithaco 1201), with a gain typically of 100. The signal was digitized with a Tektronix RTD 710 and read into the computer (HP 340) for analysis. A photoacoustic reference is an inert absorber that degrades all absorbed photons to heat in a time shorter than the PA resolving time. Two types of photoacoustic reference were used: (1) the internal reference was the PS I complex sample with saturated background illuminations,[32] and (2) the external reference was Sheaffer Jet black ink suspended in 10 mM HEPES (pH 8.0) buffer.

Convolution Analysis of Photoacoustic Waves. Two different convolution programs were used to analyze the photoacoustic signals generated in cyanobacterial PS I samples: (1) a photoacoustic convolution method as described elsewhere[13] and (2) a commercial software Sound Analysis (Version 1.50D) kindly provided by Dr. Small from Quantum Northwest, Inc. The results of the programs agreed within the rather large errors of the analysis.

(10) Rudzki, S. J.; Libertini, L. J.; Small, E. W. *Biophys. Chem*. **1992**, *42*, 29−48.
(11) Feitelson, J.; Mauzerall, D. *J. Phys. Chem.* **1996**, *100*, 7698−703.
(12) Zhang, D.; Mauzerall, D. *Biophys. J.* **1996**, *71*, 381−388.
(13) Feitelson, J.; Mauzerall, D. *J. Phys. Chem. B* **2002**, *106*, 9674−9678.
(14) Arata, H.; Parson, W. *Biochim. Biophys. Acta* **1981**, *636*, 70−81.
(15) Delosme, R.; Beal, D.; Joliot, P. *Biochim. Biophys. Acta* **1994**, *1185*, 56−64.
(16) Nagy, L.; Kiss, V.; Brumfeld, V.; Malkin, S. *Photochem. Photobiol*. **2001**, *74*, 81−87.
(17) Edens, G. J.; Gunner, M. R.; Xu, Q.; Mauzerall, D. *J. Am. Chem. Soc*. **2000**, *122*, 1479−1485.
(18) Hou, J.-M.; Boichenko, V. A.; Wang, Y.-C.; Chitnis, P. R.; Mauzerall, D. *Biochemistry* **2001**, *40*, 7109−7116.
(19) Hou, J. M.; Boichenko, V. A.; Diner, B. A.; Mauzerall, D. *Biochemistry* **2001**, *40*, 7117−7125.
(20) Boichenko, V. A.; Hou, J.-M.; Mauzerall, D. *Biochemistry* **2001**, *40*, 7126−7132.
(21) Herbert, S. K.; Han, T.; Vogelmann, T. C. *Photosynth. Res.* **2001**, *66*, 13−31.
(22) Mauzerall, D.; Hou, J.-M.; Boichenko, V. A. *Photosynth. Res.* **2002**, *74*, 173−180.
(23) Losi, A.; Yruela, I.; Reus, M.; Holzwarth, A. R.; Braslavsky, S. E. *Photochem. Photobiol. Sci*. **2003**, *2*, 722−729.
(24) Delosme, R. *Photosynth. Res.* **2003**, *76*, 289−301.
(25) Brettel, K.; Vos, M. H. *FEBS Lett*. **1999**, *447*, 315−317.
(26) Shinkarev, V. P.; Vassiliev, I. R.; Golbeck, J. H. *Biophys. J*. **2000**, *78*, 363−372.
(27) Setif, P.; Brettel, K. *Biochemistry* **1993**, *32*, 7846−54.
(28) Schlodder, E.; Falkenberg, K.; Gergeleit, M.; Brettel, K. *Biochemistry* **1998**, *37*, 9466−9476.
(29) Brettel, K.; Vos, M. H. *FEBS Lett.* **1999**, *447*, 315−317.
(30) Sun, J.; Ke, A.; Jin, P.; Chitnis, V. P.; Chitnis, P. R. *Methods Enzymol.* **1998**, *297*, 24−139.
(31) Johnson, T. W.; Shen, G.; Zybailov, B.; Kolling, D.; Reategui, R.; Beauparlant, S.; Vassiliev, I. R.; Bryant, D. A.; Jones, A. D.; Golbeck, J. H.; Chitnis, P. R. *J. Biol. Chem*. **2000**, *275*, 8523−8530.
(32) Malkin, S.; Cahen, D. *Photochem. Photobiol*. **1979**, *29*, 803−813.

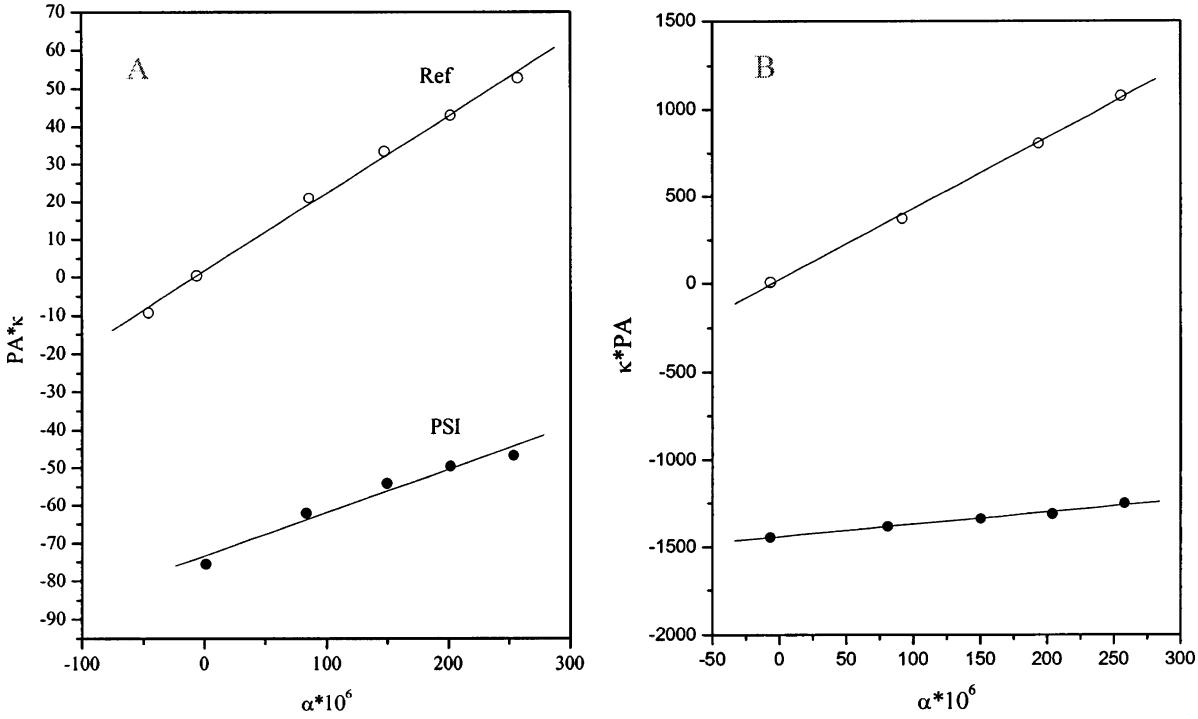

Figure 1. Peak-to-peak amplitude analysis of the nanosecond and microsecond photoacoustic data of PS I, showing similar volume changes but very different enthalpies. Conditions: pH 8.0, 10 mM HEPES, the absorbency value of PS I samples at 680 nm was ~2.0 per mm and 300 μM PMS for the 0.1 mm cell and 0.2 per mm and 160 μM PMS for the 1 mm cell, 2.0 mM sodium ascorbate (ASC), 0.03% DM, flash energy is ~3.0 μJ/cm^2, excitation at 680 nm. Panel A: nanosecond data; the upper curve is a linear fit of the PA signal for PA reference by the equation of PA*$\kappa = 1.97 + 0.241 \times 10^6\alpha$. The lower curve represents the fit of PA signals of the PS I sample by the equation of PA*$\kappa = -8.4 - 0.053 \times 10^6\alpha$. Panel B: microsecond data; the upper curve fits the PA signals of the reference by the equation of PA*$\kappa = 20.5 + 4.09 \times 10^6\alpha$. The lower curve is the PA signal from the PS I sample and is fit with the equation PA*$\kappa = -1440 + 0.705 \times 10^6\alpha$. The intercepts of the PS I sample were used to calculate the volume change, and the difference in slopes was used to calculate the thermal efficiency and enthalpy change of reaction (for details, see ref 18). The volume change ΔV and enthalpy change ΔH were listed in Table 1.

Results

Peak-to-Peak Analysis of Photoacoustic Waves. To measure the enthalpy and volume changes of charge separation in PS I forming $F_{A/B}^-$ from A_1^- from that forming $P_{700}^+A_1^-$ from the excited state of P_{700}, we extended our pulsed photoacoustic methodology to the nanosecond time scale. The pressure waves showed a half-width of ~250 ns, narrower than that (~2 μs) on the microsecond time scale. The time resolution limit depends on the S/N and is ~20 ns in this fast PA system. When the temperature is cooled to 3.8 °C, the reference photoacoustic signal decreases to zero. The expansibility of the aqueous solution is zero at this temperature, and this indicates that the fast PA system responds only to the volume change as expected. In contrast, with the purified photosystem I sample, the photoacoustic signals at both 25 and 3.8 °C showed a large negative signal, larger at the lower temperature, indicating that the volume change on charge separation in photosystem I on the nanosecond time scale, as on the microsecond time scale, is a volume contraction.[18]

We analyzed the overall photoacoustic signals (peak-to-peak value) on the nanosecond and microsecond time scales (Figure 1) according to the methodology described previously.[18] The volume contraction was -25 ± 2 A^3 on the nanosecond time scale, the same as that (-26 A^3) on the microsecond time scale within the error.[18,20] However, a low thermal efficiency (TE, $44 \pm 5\%$), which is the ratio of light energy stored in the photosystem to the absorbed light energy, was obtained on the nanosecond time scale (Figure 1A). This corresponds to a large enthalpy of -0.9 ± 0.1 eV. The TE and ΔH are dramatically different from that (76%, ΔH of -0.4 eV) of charge separation on the microsecond time scale (Figure 1B).

There are four possibilities to explain the discrepancy of the TE and enthalpy changes on the two different time scales. We will check each of these issues as follows.

First, the experimental conditions may not be optimized; for example, the concentration (~600 μM) of electron donor/acceptor phenazine methosulfate (PMS) in the nanosecond cell may be too high as compared to that in the microsecond cell (~160 μM). This could induce unexpected side-reactions in PS I as PMS can serve as both an acceptor and a donor and is highly chemically reactive. We varied the concentration of PMS from 600 to 300 μM in the nanosecond cell. The volume change and thermal efficiency of charge separation were the same, indicating that the low thermal efficiency is not due to the concentration of PMS.

Second, the quantum yield of chemistry may not be ~100% but only ~50%. To test the quantum yield in the PS I samples, we measured the volume change and thermal efficiency on the microsecond time scale using the same experimental conditions as reported previously where we showed that the quantum yield was 1.[18] The same thermodynamic parameters were observed on these preparations as those reported previously, and thus the quantum yield is close to 100%.

Third, the concentration of PS I trimer on the nanosecond time scale is ~10 times higher than that on the microsecond time scale because of the shorter path length. This may affect the state of PS I centers; for example, aggregation may occur. The state of PS I may be different from that of dilute PS I

samples. We used the PS I trimer sample with the same high concentration (~2.0 A_{680}/mm) and directly measured the volume change and thermal efficiency of photoreaction on the microsecond time scale. The large negative volume (−25 A^3) and high thermal efficiency (78%) were obtained. These values are the same as those (−26 A^3 and 76%) of the dilute PS I samples with an A_{680} of ~0.2/mm. Thus, the state of PS I at high concentration has no effect.

Finally, the measurement system of nanosecond photoacoustic apparatus may not be optimized, and there is always the possibility of systematic error. To verify the validity of our nanosecond photoacoustic apparatus, we chose the *menA*$^-$ and *menB*$^-$ PS I mutants of *Synechocystis* 6803. In these two mutants, the genes of *menA*$^-$ or *menB*$^-$ that are responsible for the biosynthesis of phylloquinone are deleted.[31] As a result, the native phylloquinone (A_1) in PS I of both mutants was missing. Multiple spectroscopic techniques revealed that a foreign plastoquinone (A_P) is recruited into the A_1 site.[33−35] One of the most interesting features is that the kinetics of electron transfer from A_P to F_X are slowed 1000-times from 20−200 ns to 15−300 μs.[33−35] The microsecond photoacoustic system has a time window of 0.1−10 μs with a time resolution of ~50 ns and the nanosecond photoacoustic apparatus with a window of 0.02−1 μs with a time resolution of ~20 ns. Thus, using these two different photoacoustic setups would be expected to give identical results, as there are no kinetic components between 10 ns and 10 μs in the *menA*$^-$ and *menB*$^-$ mutant PS I's. The observed results on these two mutants on both time scales (data not shown, to be published) indeed revealed the same volume change (−17 ± 2 A^3) and thermal efficiency (60 ± 5%, ΔH of −0.7 eV) as those measured in the first step of the WT reaction. This excludes the possibility of systematic error in the nanosecond PA measurements.

Therefore, we conclude that the enthalpy of charge separation in PS I of *Synechocystis* 6803 on the nanosecond time scale is truly large and negative using the peak-to-peak analysis. This result implies that the electron-transfer steps, that is, P_{700} to A_1 and A_1^- to $F_{A/B}$, may have dramatically different enthalpy changes with the second step being positive.

Convolution Analysis of Photoacoustic Waves. The convolution analysis on photoacoustic data allows one to time-resolve the individual step of photoreaction.[10,13] The convolution analysis on the nanosecond photoacoustic data is shown in Figure 2A. We are able to resolve one lifetime of ~100 ns (curve 3) and a prompt component of <20 ns (curve 2). The lifetimes on adding a second component were not reproducible: there may well be a distribution of time constants. The amplitude analysis of the nanosecond PA signal is shown in Figure 2B. The molecular volume change and enthalpy changes are summarized in Table 1. The prompt component is assigned to the charge separation for the formation of $P_{700}^+A_1^-$ from excited-state P_{700}*, which takes place in picoseconds, faster than the time resolution. The volume contraction of the charge separation is −21 ± 2 A^3, and the enthalpy change is −0.83

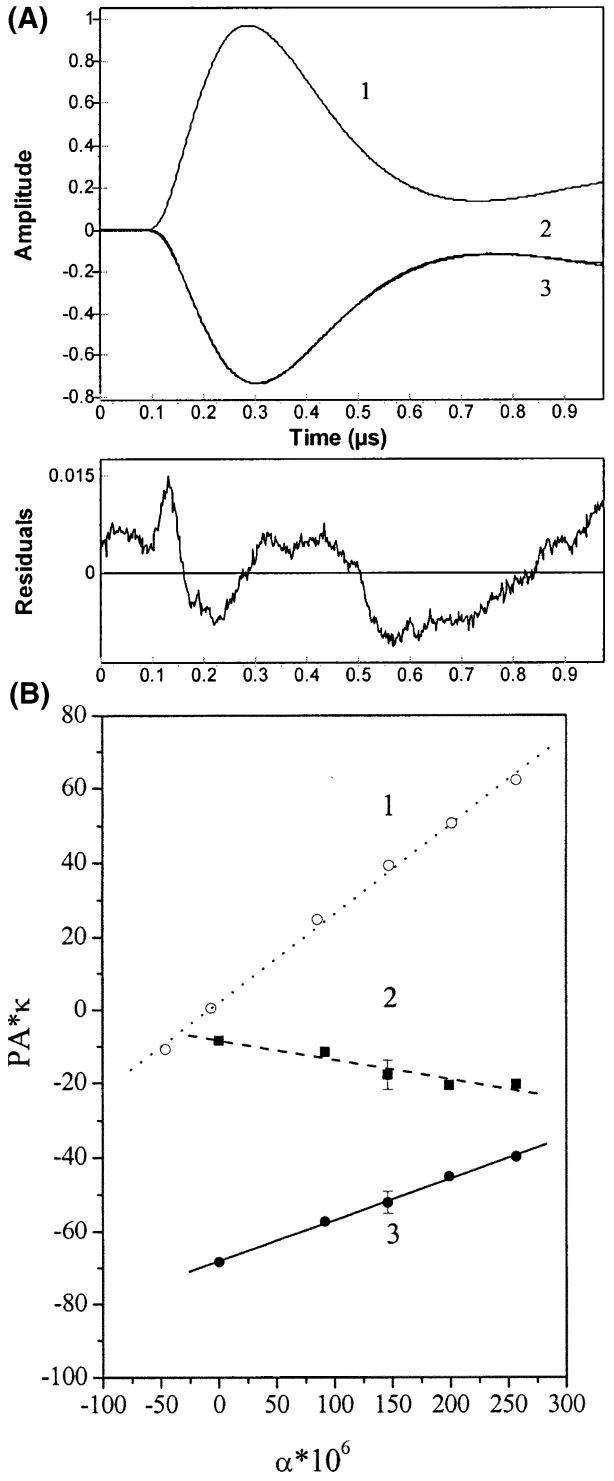

Figure 2. (A) Convolution fit of a typical nanosecond photoacoustic pressure wave of PS I via the PA cell path of 0.10 mm. Upper panel: curve 1 is a photoacoustic reference signal at 25 °C. Curve 2: observed photoacoustic signal of photosystem I center at 25 °C. Curve 3: simulation by two components, t_0 < 20 ns with relative amplitude $A_0 = -0.67$ and t_1 = 100 ns with $A_1 = -0.14$. Lower panel: amplified scale of residues of the simulation, average value ±0.5%. Sample conditions: the absorbency of photosystem I sample or photoacoustic black ink was 2.0 per mm at 680 nm, 10 mM HEPES, pH 8.0, 0.03% DM, flash energy at ~3.0 μJ cm^{-2}, 160 μM PMS. (B) Plots of amplitude times compressibility versus expansivity. Curve 1 is the reference. Curve 2 is the ~100 ns component showing positive enthalpy and small volume change. Curve 3 is the prompt component with larger negative enthalpy and large volume change. The enthalpies and volume changes are listed in Table 1.

(33) Zybailov, B.; Van der Est, A.; Zech, S. G.; Teutloff, C.; Johnson, T. W.; Shen, G.; Bittl, R.; Stehlik, D.; Chitnis, P. R.; Golbeck, J. H. *J. Biol. Chem.* **2000**, *275*, 8531−8539.
(34) Semenov, A. Yu.; Vassiliev, I. R.; Van der Est, A.; Mamedov, M. D.; Zybailov, B.; Shen, G.; Stehlik, D.; Diner, B. A.; Chitnis, P. R.; Golbeck, J. H. *J. Biol. Chem.* **2000**, *275*, 23429−23438.
(35) Johnson, T. W.; Zybailov, B.; Jones, A. D.; Bittl, R.; Zech, S.; Stehlik, D.; Golbeck, J. H.; Chitnis, P. R. *J. Biol. Chem.* **2001**, *276*, 39512−39521.

Table 1. The Molecular Volume and Enthalpy Changes of Charge Separation Revealed by Convolution Analysis of Photoacoustic Waves of PS I Trimers from *Synechocystis* sp. PCC 6803

				τ_1 (<10 ns)[c]		τ_2 (~200 ns)	
time scales	PMS[a] (μM)	OD_{680}[b] (/mm)	Ea (μJ/cm^2)	ΔV (A^3)	ΔH (eV)	ΔV (A^3)	ΔH (eV)
nanosecond	60	~2.0	~3.0	-21 ± 2	-0.83 ± 0.10	-3.5 ± 1.5	$+0.35 \pm 0.2$
microsecond	300	~0.20	~1.0	-24 ± 2	-0.80 ± 0.10	-3 ± 2	$+0.4 \pm 0.3$

[a] Other conditions are pH 8.0, 10 mM HEPES, 0.03% DM, and 2 mM ASC. [b] The OD_{680} of 0.20/mm of the PS I sample is equivalent to 16 μM Chl. [c] The time resolution limit for the microsecond photoacoustics is ~50 ns.

eV. The ~100 ns component is attributed to the A^-F_X to $F_{A/B}$ step, following the format of Santabara et al.[9] Its volume change is -3.5 ± 1.5 A^3. The most interesting finding is that the enthalpy change associated with this step is positive, $+0.35 \pm 0.20$ eV. The solution cools during the reaction. The data are summarized in Table 1.

To confirm these results, we also analyzed the microsecond time scale data by convolution (Figure 3A). The typical residues for fitting the photoacoustic waves are small (<±2%) and gave evidence of a fractional microsecond component with positive enthalpy. However, the changes of the time constants with temperature had limited reproducibility. Once again, we resolved a component with a lifetime of ~500 ns at 3.8 °C and a fast component (<~50 ns). A halftime longer than that found on the nanosecond time scale is expected because of the lower temperature, and, from a distribution of time constants, the slower scale weights the longer halftimes. The amplitudes are plotted in Figure 3B. As is shown in Table 1, the prompt component (<50 ns) has a large enthalpy change of -0.8 ± 0.20 eV and a volume change of -24 ± 2 A^3. In contrast, the ~500 ns component has a small volume change (-3 ± 2.0 A^3) and a positive enthalpy change ($\Delta H = +0.4 \pm 0.30$ eV) quite consistent with the nanosecond results within the large errors.

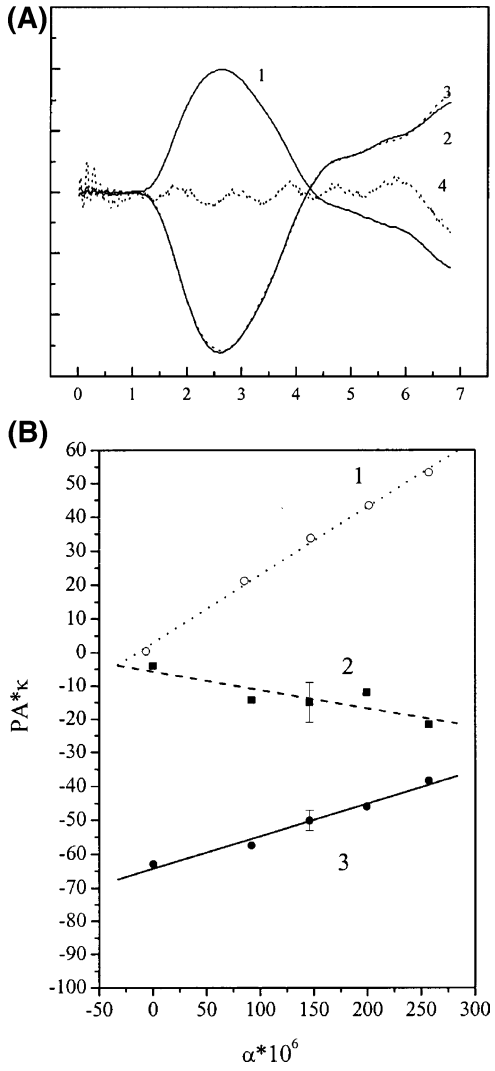

Figure 3. (A) Convolution fit of a typical microsecond photoacoustic pressure wave of PS I via the PA cell path of 1.0 mm. Curve 1: photoacoustic reference signal at 25 °C. Curve 2: observed photoacoustic signal of photosystem I center at 3.8 °C. Curve 3: convolution fit of experimental data: prompt amplitude −1.25, amplitude of the 500 ns component, −0.1. Curve 4: the residues of the fit multiplied by a factor of 5. Sample conditions: the absorbency of photosystem I sample or photoacoustic black ink was 0.20 per mm at 680 nm, 10 mM HEPES, pH 8.0, 0.03% DM, flash energy at ~1.0 μJ cm^{-2}. (B) Plots of amplitude times compressibility versus expansivity. Curve 1 is the reference. Curve 2 is the 500 ns component showing positive enthalpy and small volume change. Curve 3 is the prompt component with larger negative enthalpy and large volume change. The enthalpies and volume changes are listed in Table 1.

Discussion

Using pulsed time-resolved photoacoustic spectroscopy, the thermodynamic parameters of electron-transfer reactions have been measured in bacterial photosynthesis and oxygenic photosynthesis,[14−24] as well as in chemical solutions[10−13] and photobiological systems.[36−38] The accessible thermodynamics parameters are the molecular volume change (e.g., electrostriction or conformational change), enthalpy, and, assuming the free energy changes are known, entropy changes, associated with the individual photoreaction steps. In previous work, we have measured volume change (−26 A^3) and enthalpy change (−0.4 eV) of charge separation in photosystem I of *Synechocystis* 6803 on the microsecond time scale.[18] These values are similar to those in the bacterial reaction center from *Rb. sphaeroides*.[17] In contrast, these parameters in photosystem II of *Synechocystis* 6803 are dramatically different with a small volume change (~ −3 to −10 A^3) and a large negative enthalpy change (−1.1 eV).[19] These measurements provide important and insightful information on thermodynamics of electron transfer in biological systems. They reveal that the driving force in the photosynthetic reactions may be both enthalpic and entropic. However, most of the thermodynamic parameters using photoacoustics are on the1-μs time scale. To obtain detailed information on intermediates in the PS I reactions, we measured the volume change and enthalpy change on the nanosecond time scale.

(36) Strassburger, J. M.; Gartner, W.; Braslavsky, S. E. *Biophys. J.* **1997**, *72*, 2294−2303.
(37) Losi, A.; Wegener, A. A.; Engelhard, M.; Braslavsky, S. E. *J. Am. Chem. Soc.* **2001**, *123*, 1766−1767.
(38) Nishioku, Y.; Nakagawa, M.; Tsuda, M.; Terazima, M. *Biophys. J.* **2002**, *83*, 1136−1146.

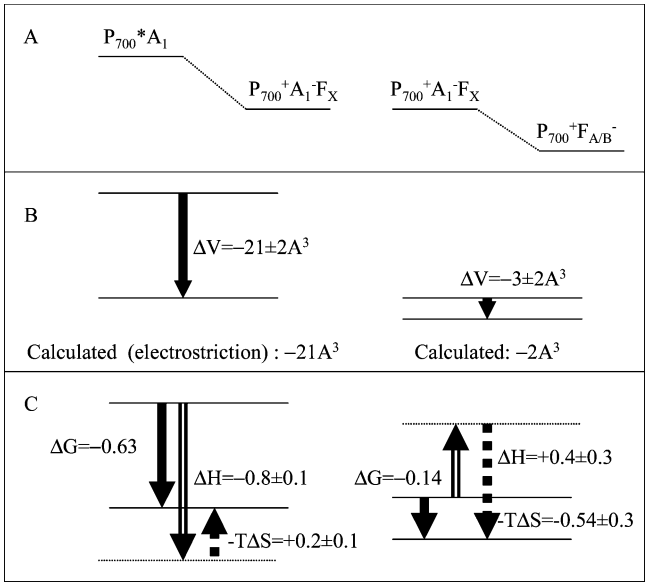

Figure 4. Thermodynamic and kinetic assignments of photoacoustic measurements in PS I of *Synechocystis* sp. PCC 6803. Panel A: Assignment of possible electron transfer reactions. Panel B: Volume contractions obtained experimentally and calculated using eq 1. Panel C: Thermodynamic parameters of electron-transfer reactions in PS I. Closed arrows are the volume changes in panel B and the free energies in panel C, open arrows stand for the enthalpy changes obtained in this work, and dashed arrows refer to the entropy changes calculated using the Gibbs relation: $\Delta G = \Delta H - T\Delta S$. The free energy is the difference of the redox potentials of the cofactors given in a previous publication.[8,9]

Volume Contraction via Electrostriction. The intrinsic molecular volume change of photoreaction in biological systems arises from two different causes: (1) electrostriction effect and (2) protein volume conformational change.

The volume contraction caused by electrostriction can be calculated using the modified Drude−Nerst equation:[22]

$$\Delta V_{el} = \frac{\partial \Delta G_{el}}{\partial P} = \left(\frac{e^2\kappa}{2\epsilon}\right) \times \left(\frac{\partial \ln \epsilon}{\partial \ln V}\right) \times \left[\frac{z_+^2}{r_+} + \frac{z_-^2}{r_-} + \frac{2z_+z_-}{r_\pm}\right] \quad (1)$$

where ΔV_{el} is electrostriction, ΔG_{el} is the Born charging energy, P is pressure, z_+ and z_- are the signed charge on the positive and negative ions, κ is compressibility of the protein, V is its molar volume, ϵ is its dielectric coefficient or relative permeability, r_+ and r_- are the radii of the donor and acceptor (assumed previously neutral), and $r_\pm$ is the distance between the two ions.

The volume changes of charge separation in photosystem I of *Synechocystis* 6803 are summarized in Table 1 and Figure 4. We are able to measure the early step of photoreaction in PS I producing $P_{700}^+ A_1^-$ from P_{700}*, which is associated with a volume contraction of -22 ± 2 A^3. Assuming the radii of A_1 (4 A) and P_{700} (7.5 A), separated by ~30 A, a volume change of -21 A^3 was calculated (Figure 4), which is reasonably close to the measured value. The parameters used are given in Hou et al.[18] and Mauzerall et al.[22] The following electron-transfer reaction from A_1^- to $F_{A/B}$ produces a small volume change of -3 ± 2 A^3. We calculated the volume change from A_1^- to $F_{A/B}$ to be -2 A^3 (Figure 4). The overall step for producing $P_{700}^+F_{A/B}^-$ from excited-state P_{700}* is $-22 + (-3) = -25$ A^3, which agrees well with the previously observed value (-26 ± 1 A^3) for the same preparations using microsecond PA methodology.[18] Using eq 1, we calculate a value of -26 A^3, the same as that observed experimentally, if we assume that the acceptor ($F_{A/B}$) is a super-complex $(Fe_4S_4)(Cys_4)$ with a charge change from -1 to -2 and radius of 8 A. The detailed calculation and discussion have been published.[22]

The volume change of the photoreaction could be also caused by a particular kind of conformational change, which creates or destroys volume. Such conformational changes were observed during the photoreaction of bacteriorhodopsin and bovine rhodopsin.[36−38] However, the observed data of volume contraction in photosynthetic reaction centers are fit well with the Drude−Nernst equation,[22,39] suggesting that the protein structure in these centers is fairly rigid and there is probably no significant conformational change during the initial charge separation reaction in PS I centers. This is consistent with the fact that these primary electron-transfer reactions can occur at cryogenic temperatures.

Free Energy, Enthalpy, and Entropy. Thermodynamic parameters such as the free energy (redox potential of cofactors in situ), enthalpy, and entropy are crucial information to fully understand the reaction mechanism of electron transfer at the molecular level. The thermodynamics of electron transfer in biological system have been of great interest during the past decade, and the accumulated evidence supports the view that the entropy changes in electron- and proton-transfer reactions in chemical and biological system are significant and cannot be neglected.[17−20,40,41]

We summarize the free energy, enthalpy, and entropy changes of PS I in Figure 4. The solid arrows are the free energies of reaction obtained from the redox potentials of cofactors in situ, the open arrows are the enthalpy changes observed by means of photoacoustic data, and the dashed arrows are the calculated entropy changes using the Gibbs relation $\Delta G = \Delta H - T\Delta S$. A discussion of errors in the estimates of free energy will be given soon by Mauzerall. They include the fact of the long time scale of electrochemical measurements and of measuring only a single one of the pair of redox partners, thus neglecting any interaction between them. We will use the free energy compilation of Santabara et al., but none of our conclusions are critically dependent on the exact values used. The alternative free energies increase the magnitude of the enthalpies and entropies. Taking the redox potential of A_1F_X (-0.67 V) and P_{700} ($+0.47$ V) and the trap energy of P_{700}* (1.77 eV), the free energy for the early step of electron transfer forming $P_{700}^+ A_1^-F_X$ from P_{700}* is -0.63 eV. The convolution fits on both the nanosecond and the microsecond time scales show an enthalpy change of -0.8 ± 0.1 eV (Table 1), and thus the apparent entropy change is negative, -0.2 ± 0.1 eV. All entropies will be quoted as $T\Delta S$ with $T = 25$ °C. The following step is the electron-transfer reaction from $A_1^-F_X$ to $F_{A/B}$, with relatively small free energy, -0.14 eV. The enthalpy change for this step revealed by convolution is positive, $+0.4 \pm 0.3$ eV (Table 1). The apparent entropy change for this step is $+0.54 \pm 0.3$ eV, large and positive, but with considerable error. This entropy is larger than that of the free energy. We conclude that the A^-F_X to $F_{A/B}$ step in cyanobacterial photosystem I is entropy driven. PS I releases significant energy of the exciting light as heat into the

(39) Drude, P.; Nernst, W. *Z. Phys. Chem.* **1894**, *15*, 79−85.
(40) Woodbury, N. W.; Allen, J. P. In *Anoxygenic photosynthetic bacteria*; Blankenship, R. E., Madigan, M. T., Bauer, C. E., Eds.; Kluwer Academic Publishers: Norwell, MA, 1995; pp 527−557.
(41) Xu, Q.; Gunner, M. R. *J. Phys. Chem. B* **2000**, *104*, 8035−8043.

environment but stores energy as negative entropy in the early steps of electron transfer in the PS I system. This is followed by absorption of heat from the environment, a positive enthalpy, driven by release of positive entropy in the second electron-transfer step. Thus, the thermodynamics of charge separation in protein systems can be more complex than anticipated. In some cases, enthalpy contribution predominates in the free energy and the entropy component is small. In other cases, both enthalpy and entropy may play roles in the electron-transfer reaction. In this work, the experimental data show that in the case of the A^-F_X to $F_{A/B}$ step in cyanobacterial PS I the entropy component is the driving force.

Given the unusual result of these measurements, we must see if other explanations can be found. The spread of time constants for the A_1^- to F_{AB} reaction has been explained as alternate paths along the symmetric A and B chains of acceptors.[6] If the fraction of a given path were temperature dependent, then the measured amplitudes of the PA signals could be contaminated by this change. Note that this would require that the enthalpy of the two paths differ substantially. If they are the same, then varying their proportions will have no effect. The data of Agalarov and Brettel are ambiguous on this matter.[42] On fitting their reduction kinetics of A_1 with two exponentials, the thermal effect on the amplitudes over our 20 °C range is negligible (their Figure 2B). However, a better fit with three exponentials shows large thermal effects on the "fixed" (300 ns) and "slow" (1 μs) components (their Figure 2D). The effects are in opposite directions with almost equal amplitudes, suggesting a fitting problem. The "fixed" component would appear as a positive enthalpy in our plots, but the value of the component amplitudes indicates that the effect would be to decrease the observed positive enthalpy by <0.2 eV. The slow component would actually increase the positive enthalpy by about the same amount. Correction for the reduced amplitude of the slow component in the PA measurements would increase their values by ~30%. Given these ambiguities, we prefer to adopt the simplest hypothesis that the slow components of the $A_1^-F_X$ to F_{AB} reaction have the large positive enthalpy quoted in Table 1 with appropriate errors. Because we cannot resolve the fast component of smaller amplitude of this reaction from the faster P_{700}* to A_1 reaction, we cannot state its enthalpy.

Another source of complication in the electron-transfer kinetics is the ensuing transfers from F_X to F_A and then to F_B. The time constants for these reactions are about the same as those quoted above for the fast and slow A_1 reduction, with F_X to F_A being slower. Thus, we cannot distinguish between the various FeS complexes, and that is why we refer to them as $F_{A/B}$. There may be an equilibrium among the FeS clusters as is strongly argued by Santabara et al., in which case some of the enthalpy measured may be that of the equilibrium, not of a single electron-transfer step.[9] This in no way changes our basic thermodynamic argument. A measured step of the reaction has a large positive enthalpy, and because the free energy differences are small, particularly for an observable equilibrium (~0.1 eV), it must also have a large, positive entropy.

The redox thermodynamics of many FeS proteins (ferrodoxins) have been determined.[43] Interestingly, most of the Fe_4S_4-$(Cys)_4$ proteins have positive enthalpies of reduction of +0.3 to +0.4 eV, while the others have very small negative enthalpies. The authors explain the enthalpies in terms of electrostatic interactions with the protein dipoles. All of the reduction entropies are negative as anticipated from the increase in charge and seem to vary in magnitude opposite from the enthalpies. Thus, the positive enthalpy of the $A_1^-F_X$ to F_{AB} reaction may be assigned in part to the FeS cluster reduction. The positive entropy may have contributions from the freeing of oriented polar groups on quinone anion oxidation. The previous step has a negative entropy as expected.

Entropy-driven reactions are of inherent interest because the majority of reactions are well explained simply in terms of energetics, that is, changes in enthalpy. Entropy-driven reactions have a larger positive entropy than the positive enthalpy, thus forming the required negative free energy. Statistical mechanics explains this as a large increase in the number of available states in the products relative to the reactants. Examples are the denaturation of proteins or the dissolving of ammonium nitrate in water. Sturtevant gave an analysis of the causes of large entropy changes involving proteins.[44] Of the half-dozen effects he considered, the hydrophobic effect and changes in low frequency vibrations are likely the most important. Conformation changes very likely make their largest contributions through vibrational effects. An example of a reaction claimed to be entropy driven by the hydrophobic effect is the assembly of the heptameric co-chaperonin protein 10.[45] The present simpler system is most likely explained by the vibrational effect. This can be ascribed to the loosening of the structure because of loss of charge or of the movement of a protein helix away from other helices and the ensuing decrease in interaction of the side chains. Because the electrostrictive volume changes in this step are small (Figure 4), the conformation change is favored. The less hindered movements of the side chains will add lower frequency vibrations. When their frequencies are in the range of kT/h, they much increase the number of available states at a given temperature. We estimate that a dozen such low-frequency vibrations would explain the observed entropy change. We note that F_X is at the interface of PsaA/B and PsaC components of PS I. It is thus at the correct position for protein movement.

Pulsed direct photopressure spectroscopy on the millisecond to second time scale was recently developed in the laboratory (for methodology, see refs 46,47), and we plan to use this method to investigate the electron-transfer reactions in PS I from *Synechocystis* 6803 to uncover the thermodynamics of these slower steps.

Acknowledgment. This work was supported by past grants from the National Science Foundation (MCB-9904522) and the National Institutes of Health (GM 25693) to D.M., and by a start-up fund from Gonzaga University to H.J.M.H. We are grateful to Drs. Parag Chitnis and Huadong Tang for kindly providing photosystem I trimers of *Synechosystis* 6803 and Ms. Irene Zielinski-Large for her technical assistance.

JA054870Y

(42) Agalarov, R.; Brettel, K. *Biochim. Biophys. Acta* **2003**, *1604*, 7−12.
(43) Battistuzzi, G.; D'Onofrio, M.; Borsari, M.; Sola, M.; Macedo, A. L.; Moura, J. J.; Rodrigues, P. *J. Biol. Inorg. Chem.* **2000**, *5*, 748−60.
(44) Sturtevant, J. M. *Proc. Natl. Acad. Sci. U.S.A.* **1977**, *74*, 2236−2240.
(45) Luke, K.; Apiyo, D.; Wuttung-Stafshede, P. *Biophys. J.* **2005**, *89*, 3332−3336.
(46) Mauzerall, D.; Liu, Y.; Edens, G. J.; Grzymski, J. *Photochem. Photobiol. Sci.* **2003**, *2*, 788−790.
(47) Edens, G. J.; Liu, Y.; Grzymski, J.; Mauzerall, D. *Rev. Sci. Instrum.* **2003**, *74*, 2523−2529.